Desalination and Water Treatment
www.deswater.com

17 (2010) 37–44
May

1944-3994/1944-3986
doi: 10.5004/dwt.2010.1696

Mechanical properties of microporous foams of biodegradable plastic

Takaaki Tanaka[a*], Takashi Aoki[a], Tomoaki Kouya[a], Masayuki Taniguchi[a], Wataru Ogawa[b], Yuuji Tanabe[b], Douglas R. Lloyd[c]

[a]*Department of Materials Science and Technology, Niigata University, Niigata 950-2181, Japan*
Tel. +81252627495; Fax +81252627495; email: tctanaka@eng.niigata-u.ac.jp
[b]*Department of Mechanical and Production Engineering, Niigata University, Niigata 950-2181, Japan*
[c]*Department of Chemical Engineering, The University of Texas at Austin, TX 78712, USA*

Received 31 July 2009; accepted 3 December 2009

ABSTRACT

Permeable microporous foams and membranes of biodegradable polyesters are currently used in the area of tissue engineering and drug delivery systems. Their mechanical properties are useful in the medical applications. The foams should mechanically fit to the tissues where the foams were implanted. In this study, we investigated the mechanical properties of the foams of biodegradable polyesters by compression tests. Microporous foams of poly(L-lactic acid), poly (ε-caprolactone), and poly(3-hydroxybutyrate-co-3-hydroxyvalerate) were prepared by thermally induced phase separation method. The compression tests were performed at 23–24°C with a universal testing machine. The structure of the microporous foams depended on the kinds of polymers, polymer concentrations, and quenching temperatures. The cell size of the foams was smaller when the polymer concentration was higher or the quenching temperature was lower. We analyzed the stress–strain diagrams of the foams in the compression test. The lower the relative density of the foams to the solid materials the lower the elastic limit stress was. The relative Young's modulus and relative elastic limit stress of the foams were approximately proportional to the square of their relative density and less dependent on their cell size. The dependences were similar to those of open-cell foams of polyurethane.

Keywords: Biodegradable plastic; Microporous foam; Thermally induced phase separation; Mechanical properties; Open cell foam

1. Introduction

Permeable microporous foams of biodegradable polyesters are currently used in the area of tissue engineering [1–3] and drug delivery systems [4,5]. Although materials from animals such as gelatin [6] are prepared, the biodegradable polyesters have a merit to reduce the risk of the contamination of viruses compared to the animal origin materials. The microporous foams of biodegradable polyesters were prepared by phase separation [4], particulate-leaching [7–10], combination of freeze-drying and particulate-leaching [11], emulsion freeze-drying [12], fused deposition modeling [13], stereolithography [14], etc.

Profiles of cell proliferation and drug release are the main characteristics of the porous materials in the medical applications. In addition to them the mechanical properties of the materials are also important when they are implanted [3]. Fragile scaffold cannot protect the cells from the mechanical stress while rigid

*Corresponding author

Presented at the Fifth Conference of the Aseanian Membrane Society Aseania 2009 "Recent Progress in Membrane Science and Technology", 12–14 July 2009, Kobe, Japan.

implants will hurt soft tissues. The foams should mechanically fit to the tissues where the foams were implanted. The elasticity of the microenvironment also affects the adhesion and differentiation of stem cells [15]. Some researchers measured the mechanical properties of microporous foams of biodegradable plastics. Among them, Hou et al. [8] and Zhang et al. [9] examined the compressive modulus and yield stress of the foams prepared by particulate leaching method with a wide range of porosity. The characteristics were of open cell type foams like polyurethane foams [16].

Thermally induced phase separation method is a kind of phase separation method where the polymer solution in a diluent is cooled to induce phase separation and solidification [17–19]. Microporous foams are formed after the extraction of the diluent. Isotropic porous structures are observed while anisotropic or asymmetric ones are observed in microporous materials, such as ultrafiltration membranes, prepared by nonsolvent-induced phase separation method. The pore size can be controlled by the kinds of diluents, polymer concentration, and thermal histories in thermally induced phase separation method.

In this study, we investigated the mechanical properties of the foams of biodegradable polyesters prepared by thermally induced phase separation method by compression tests. The compressive Young's modulus and elastic limit stress ($\approx$ yield stress) of microporous foams of different kinds of biodegradable polyesters, pore sizes, and densities were compared.

2. Experimental

2.1. Materials

Poly(L-lactic acid) (PLLA) (M_w = 120,000) was a kind gift from Toyota Motor Corp. (Toyota, Japan). Poly (ϵ-caprolactone) (PCL) (M_w = 70,000–100,000) and poly(3-hydroxybutyrate-*co*-3-hydroxyvalerate) (PHBV) (3HV = 12%), were prepared purchased from Wako Pure Chemical Industries (Osaka, Japan) and Sigma-Aldrich (St. Louis, MO), respectively. 1,4-Dioxane are of analytical grade. All the chemicals were used as received.

2.2. Preparation of microporous foams

Microporous foams of biodegradable polyesters were prepared by thermally induced phase separation method [18,19]. First polymers were dissolved in 1,4-dioxane containing 13% water at 80°C. In this paper, water concentration in diluents and polymer concentrations in polymer solutions are expressed in weight percent. Then the solution was poured into a 5 mm-deep stainless mold at 80°C and kept for 15 min. The mold was quenched to 0°C, −22°C, or −196°C. The formed gel was washed with water at 0°C and then dried at room temperature. 100% polymer specimen was prepared by cooling heat-melted polymer in a stainless mold.

2.3. Scanning electron microscopy (SEM)

The foam was immersed in liquid nitrogen and then fractured. It was mounted vertically on a sample holder. The surface of the sample was coated with gold–palladium using a sputter coater (JFC-1100E, JEOL, Akishima, Japan). A SEM (JSM-5800, JEOL) with an accelerating voltage of 15 kV was used to examine the membrane cross-sections and surfaces.

2.4. Compression test

The compression tests were performed at 23–24°C with a universal testing machine (RTC-1225AS, Orientic Co.). The specimen was cut in a disc of 11 mm in diameter except 100% PHBV at 3.7 mm. Compression speed was 0.5 mm min^{-1}.

2.4. Phase separation temperature

The phase separation temperatures of the polymer solutions were measured by the method described elsewhere [19].

3. Results and discussion

3.1. Internal structure of the microporous foams of PLLA

Fig. 1 shows the internal structure of microporous foams of PLLA prepared from polymer solutions at different concentrations by ice water quenching. Inter-connected structures of the microporous foam were observed. The cell size of the foams was smaller when the polymer concentration was higher.

The phase separation temperatures of ternary mixture of PLLA and 1,4-dioxane containing 13% water were 37°C, 46°C, and 64°C at 5%, 10%, and 20% PLLA concentration, respectively [19]. The temperature was higher at a higher polymer concentration in contrast to binary mixture of polymer and diluent. It can be assumed that the pore size becomes larger at a higher polymer concentration than at a lower concentration because the phase begins to separate earlier. However, the polymer-rich phase solidifies at a higher polymer concentration faster than at a lower polymer concentration because the concentration in polymer-rich phase is higher. Thus the pore size was smaller at higher

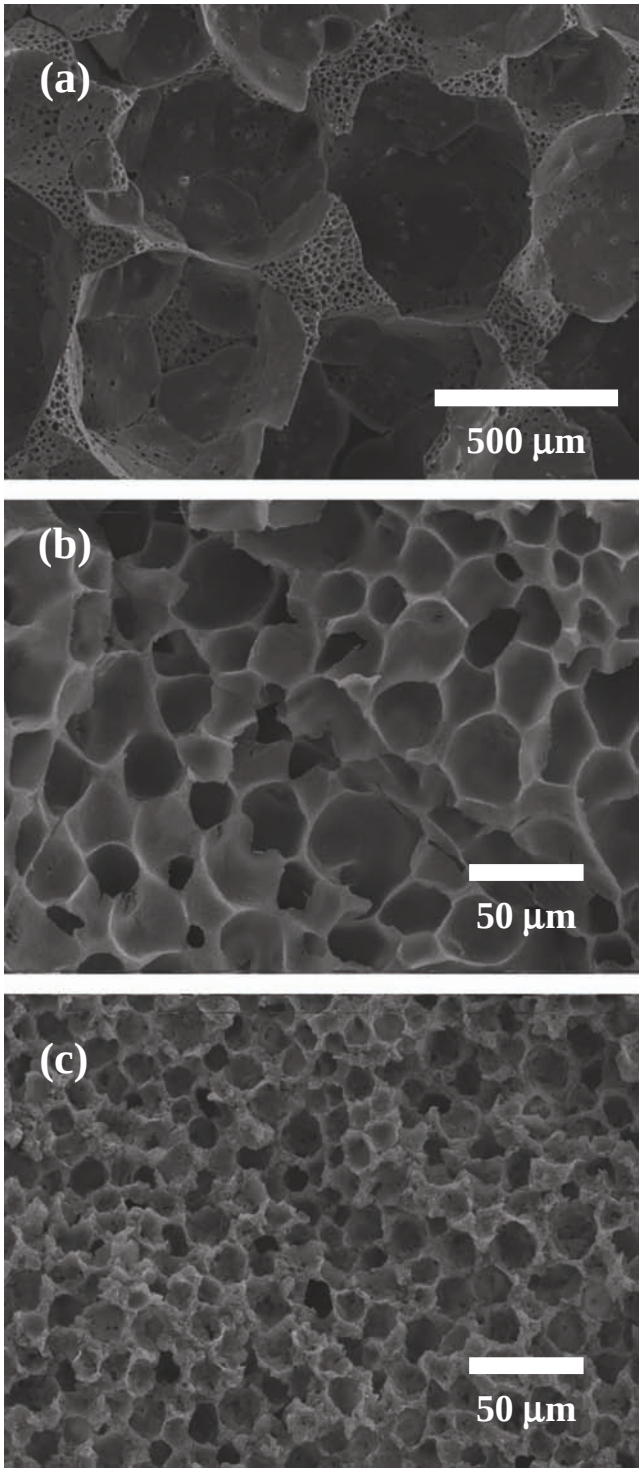

Fig. 1. Internal structures of microporous foams of PLLA prepared from polymer solutions at different polymer concentrations. The polymer solutions were quenched by ice water (0°C). Polymer concentration: (a) 5%, (b) 10%, (c) 20%.

polymer concentrations because of the short time for the growth of droplets of polymer-lean phase. The cell

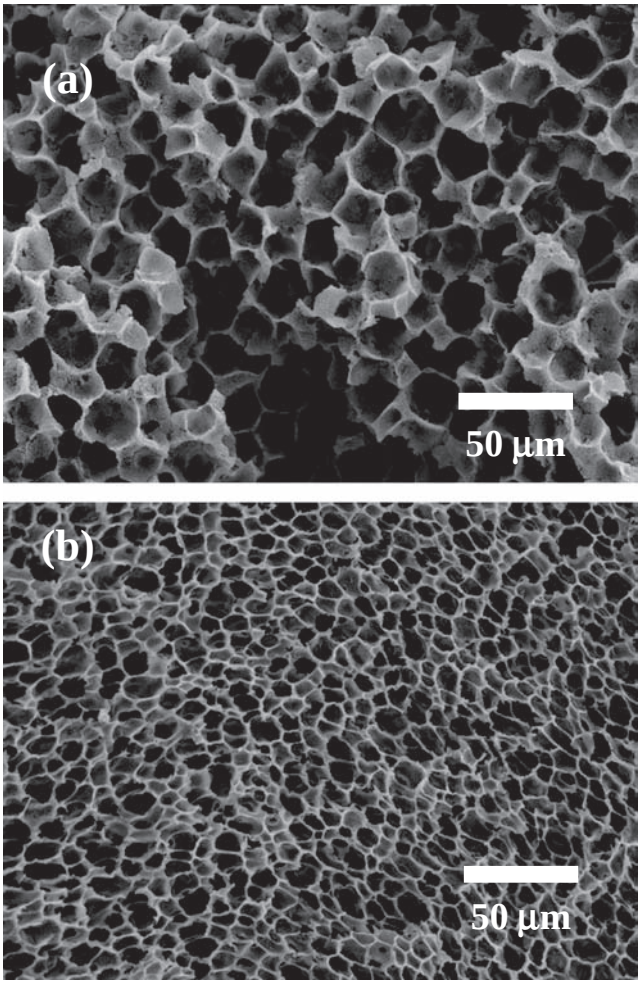

Fig. 2. Internal structures of microporous foams of PLLA prepared from polymer solutions at different quenching temperature. The polymer concentrations were 10%. Quenching temperature: (a) −22°C and (b) −196°C.

wall among the three or more cells was also porous in the foams prepared from 5% polymer solution. The secondary pores would have formed after the first phase separation for the primary pores and before solidification.

Fig. 2 shows the internal structure of microporous foams of PLLA prepared from 10% polymer solutions at different quenching temperatures. The cell size of the foams was smaller when the quenching temperature was lower (Figs. 1b, 2a, and 2b). The phase separated at the same temperature (46°C). The growth of the droplets of polymer-lean phase stopped in a shorter time because of the faster quenching (Figs. 2a and 2b). Thus the cell size became smaller. However it seems that the cell wall was not so thick prepared by the faster quenching compared to that from the polymer solution at a higher concentration by ice water quenching (Fig. 1c) while the cell size became smaller in the both

cases. The thick cell walls in Fig. 1c would be due to the higher density of the foams (see Section 3.3).

3.2. Internal structure of the microporous foams of PCL and PHBV

Fig. 3 shows the internal structure of microporous foams of PCL prepared from polymer solutions at different concentrations by ice water quenching. The cell size was larger than those of PLLA microporous foams at 10% (Figs. 1b and 3b). The phase separation temperatures of the PCL and PLLA solutions were similar [19]. However, the PCL-rich phase would solidify slower than the PLLA-rich phase because the melting point and glass transition temperature of PCL ($T_m = 60°C$ and $T_g = -60°C$) were lower than those of PLLA ($T_m = 174°C$ and $T_g = 60°C$). Thus the cells in PCL foams grew larger.

Fig. 4 shows the internal structure of microporous foams of PHBV prepared from polymer solutions at different concentrations by ice water quenching. The cell size of the PHBV foams from a 10% polymer solution (Fig. 4b) was similar to the corresponding PLLA foam (Fig. 2b). However, the PHBV foams contained leaf-like structures. The melting point, glass transition temperature, and weight average molecular weight of PHBV with hydroxyvalerate content of 12 mol% produced by Sigma-Aldrich Co. were 161°C, −2°C, and 238,000, respectively [20]. The T_m and T_g values were between PLLA and PCL. The crystal growth in polymer solution would be different between PHBV and PLLA. On the other hand the cell size became smaller at higher polymer concentrations similarly as in the PLLA and PCL foams.

The PHBV solutions were not very clear at 80°C although the solutions were clouded at room temperature. So the phase separation temperatures were not clearly measured for the PHBV solutions to analyze the formation of porous structure.

3.3. Stress–strain curves of microporous foams of biodegradable plastics

We characterized the mechanical properties of the foams by compression test. We analyzed the stress–strain diagrams of the foams (Fig. 5). The densities of the microporous foams samples were higher than the values estimated from the polymer concentrations of the solutions used for the preparation partly because the foams shrank during the preparation. The densities (ρ) were calculated from the mass, diameter, and height of the each samples before compression tests. The relative densities of the samples (ρ/ρ_s) were shown in Fig. 5. The densities of the solid sample (ρ_s) of PLLA, PCL, and PHBV were 1240, 1050, and 1180 kg m^{-3}, respectively.

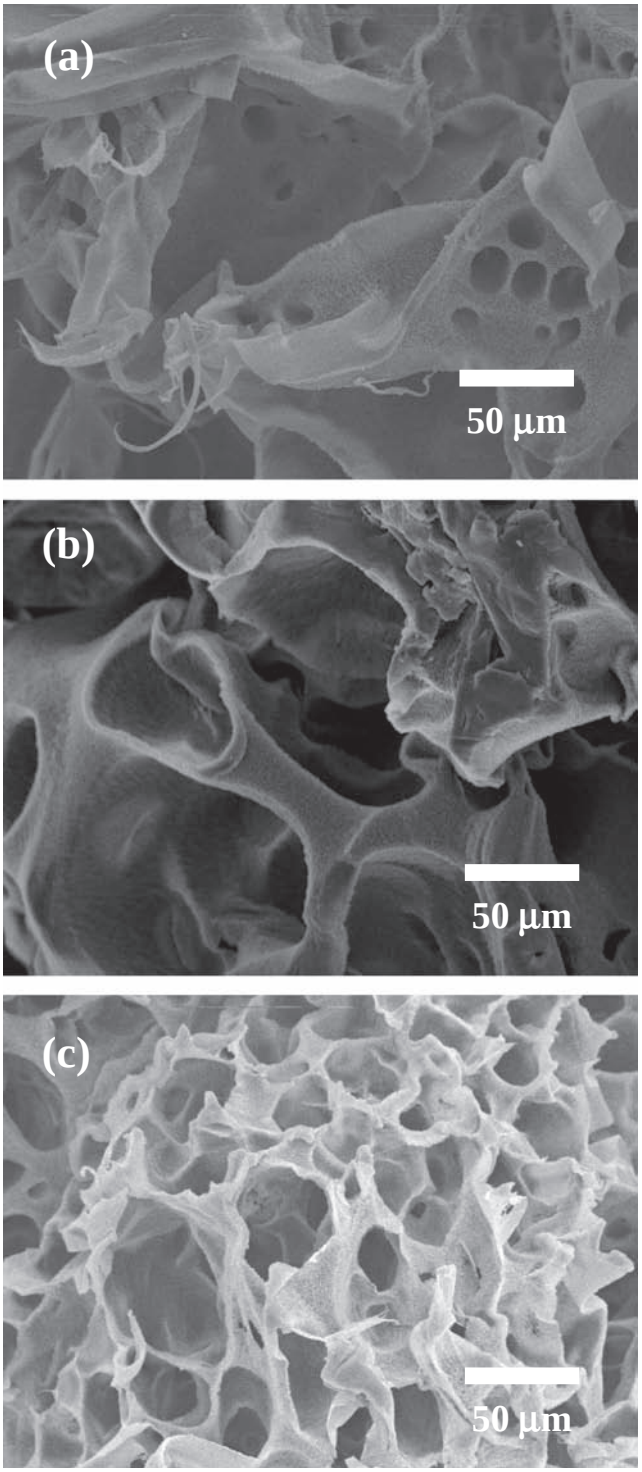

Fig. 3. Internal structures of microporous foams of PCL prepared from polymer solutions at different polymer concentrations. The polymer solutions were quenched by ice water (0°C). Polymer concentration: (a) 5%, (b) 10%, and (c) 15%.

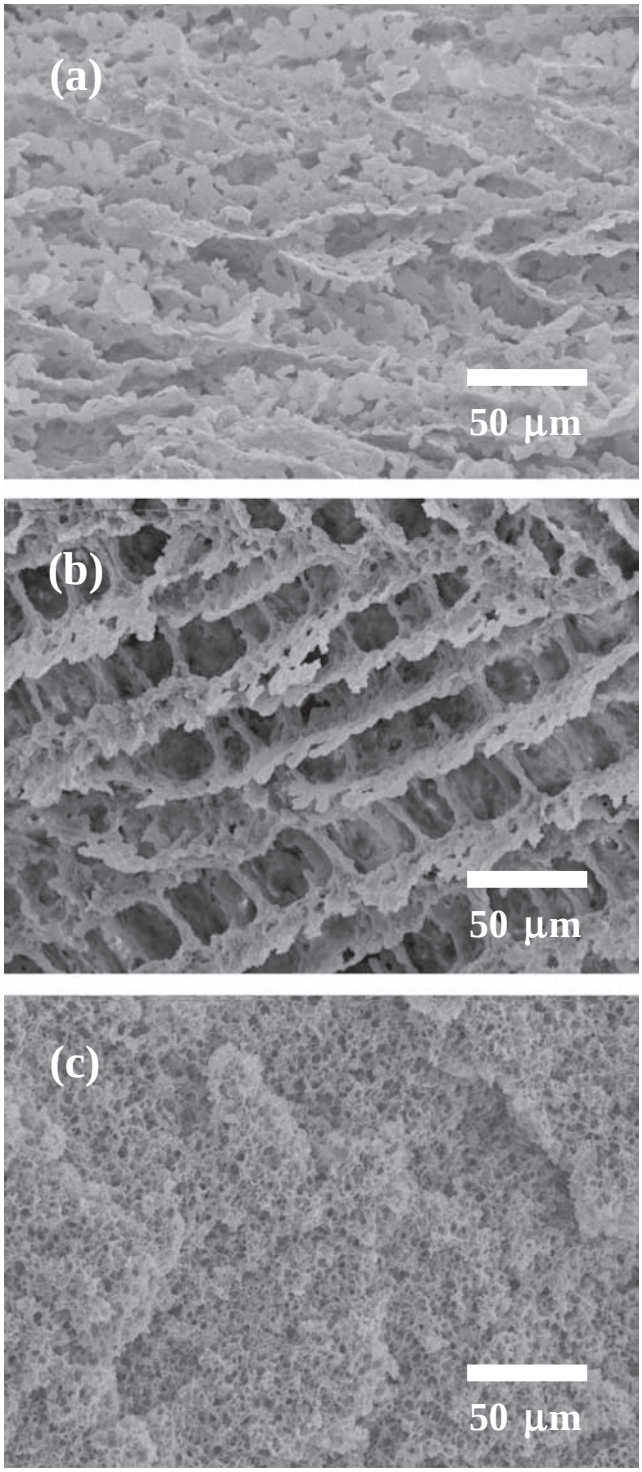

Fig. 4. Internal structures of microporous foams of PHBV prepared from polymer solutions at different polymer concentrations. The polymer solutions were quenched by ice water (0°C). Polymer concentration: (a) 5%, (b) 10%, and (c) 15%.

The initial lines of the stress–strain diagrams of the foams were not straight (Fig. 5). That would be due to

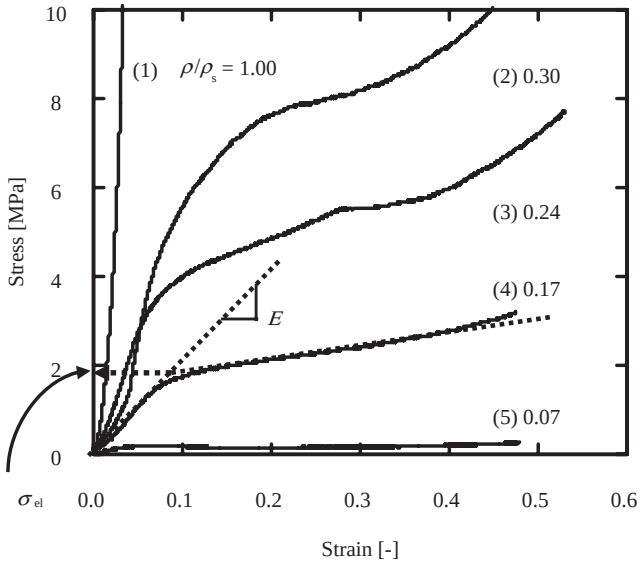

Fig. 5. Stress–strain diagram of microporous foams of PLLA. Sample (1) was prepared from heat-melted PLLA. Samples (2), (3), (4), and (5) were prepared from 20%, 15%, 10%, and 5% PLLA solutions in 1,4-dioxane containing 13% water, respectively, by quenching the solutions with ice water.

that the top and bottom surface of the specimens (Fig. 6) were not perfectly parallel. The strain was calculated from the displacement and the initial height of the specimens. The compressive Young's moduli (E) were calculated from the maximum slopes in less than 0.2 of strain.

The slope of stress–strain curve decreased largely around strain 0.1. The decrease is similar to those of the stress–strain curve of general tension tests. However, the slope increased again around 0.4 of strain. It is one of the characteristics of the stress–strain curve in the compression test of the porous materials [16]. The compressed foams begin to show the mechanical properties of the solid materials at higher strains in compression tests while the specimens are broken in general tension tests.

The stress–strain curves of the samples in this study did not show clear yielding points. Thus the elastic limit stress (σ_{el}) was estimated from the cross point of the straight line which shows the initial maximum slope and the line which shows the minimum slope around 0.2 of strain of the stress–strain curve. Elastic limit stress is a critical value where permanent deformation of materials will occur. The elastic limit stress of the solid PLLA could not be measured because of its high value. The height of the porous specimens did not recover after compression over the elastic limit strain (Fig. 6). Foams of elastic limit stress higher than the pressure at the place of implantation should be prepared to avoid the deformation of the living cells in the

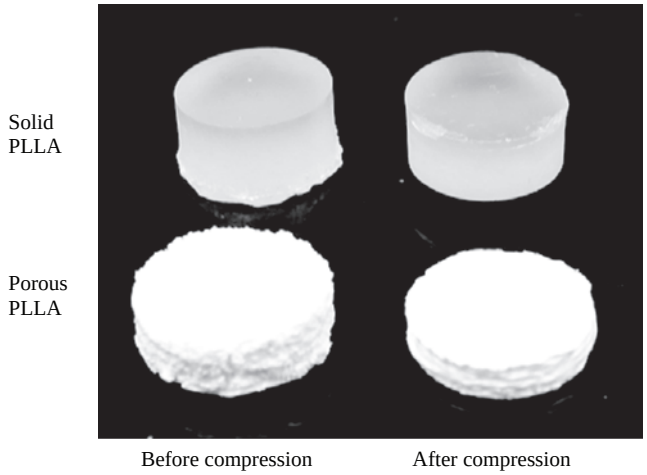

Fig. 6. Solid ($\rho/\rho_s = 1.00$) and porous ($\rho/\rho_s = 0.17$) PLLA specimens before and after compression tests.

microporous foam in tissue engineering or the excess release from the drug in drug delivery systems.

3.4. Young's modulus of biodegradable microporous foams

The relative Young's moduli of the foams were plotted against their relative density (Fig. 7). A log–log plot is usually used in the analysis of mechanical properties of foams because the slope in the plot depends on the cell structure. The theoretical slope for an ideal model of open-cell foam is 2.0 in Fig. 7 while the slope for the closed-cell foam at a relative density of 0.1 is nearly 1.0 [16]. The Young's moduli (E_s) of the solid samples of PLLA, PCL, and PHBV were 1130, 210, and 910 MPa, respectively. The relative Young's moduli (E/E_s) of microporous foams of PLLA, PCL, and PHBV were proportional to the relative density (ρ/ρ_s) to the power of 2.0, 2.4, and 2.7, respectively. Note that the data points of PLLA foams prepared by quenching at −22°C and −196°C are in the trend of PLLA foams prepared by quenching at 0°C. The cell size of PLLA foams prepared at −22°C and −196°C were much smaller than that of the foams prepared at 0°C (Figs. 1 and 2). The result in Fig. 7 implies that the relative Young's modulus of PLLA foams mainly depends on the relative density and depends less on the cell size.

Hou et al. examined the Young's moduli of the porous foams of poly(D,L-lactic acid) (PDLLA) and PCL prepared by coagulation, compression molding, and particulate leaching. The moduli were proportional to the power law. The exponents of the foams with PDLLA and PCL were 2.42 and 2.59, respectively [8].

Zhang et al. showed that the Young's modulus of the porous scaffolds with cubic and spherical macropores (355–450 μm) of poly(D,L-lactic-*co*-glycolic acid)

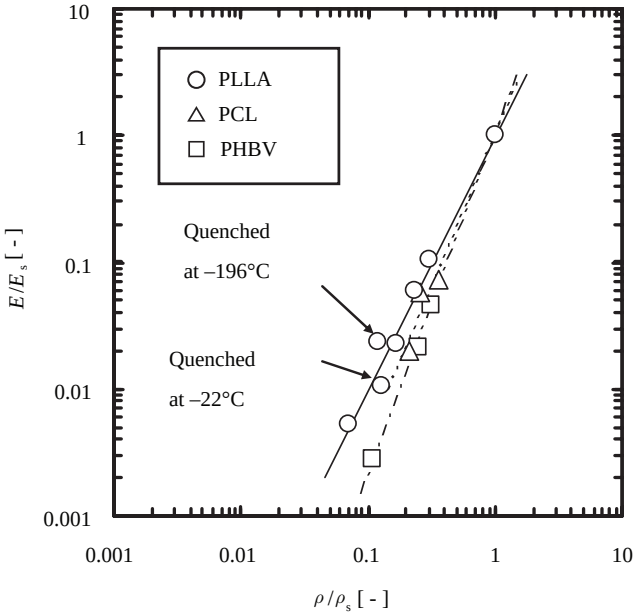

Fig. 7. Dependence of the relative Young's modulus (E/E_s) on the relative density (ρ/ρ_s) of microporous foams. The foams were prepared by quenching polymer solutions at 0°C unless otherwise noted.

(PLGA) were also proportional to the power law. The exponents of the macroporous foams with spherical and cubic pores were 2.37 and 3.13, respectively [9]. They think that the higher exponent of the foams of cubic pores is due to the defect of the pores. The foams prepared by leaching NaCl salt porogens have defects formed by the merge of two or more adjacent cubic particles. The defect effect may be more significant at low relative densities (high porosities). Thus the compressive Young's moduli of foams with cubic pores are more sensitive to those with spherical pores.

The dependences of Young's modulus on relative densities of the microporous foams were similar to those of open-cell foams of polyurethane [16]. The theoretical slope for the ideal open-cell foams in Fig. 7 is 2.0. The difference between theoretical and experimental values would be due to the structural difference of the regularly jointed beams in the theory and the open walls in the microporous foams.

3.5. Elastic limit stress of biodegradable microporous foams

The relative elastic limit stress of the foams was also approximately proportional to the square of their relative density (Fig. 8). The ratio of the elastic limit stress (σ_{el}) to the Young's modulus (E_s) of the solid materials (σ_{el}/E_s) of PLLA, PCL, and PHBV were proportional to the relative density (ρ/ρ_s) to the power of 2.1, 2.4, and 2.3, respectively. The data points of PLLA foams

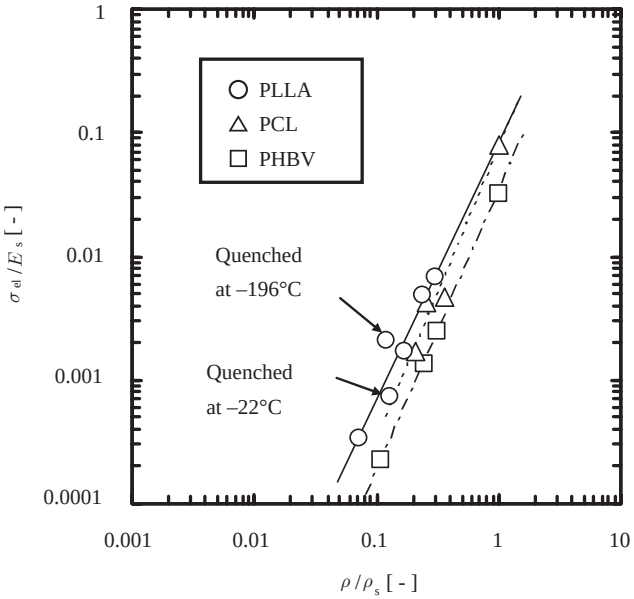

Fig. 8. Dependence of the relative elastic limit stress (σ_{el}/E_s) on the relative density (ρ/ρ_s) of microporous foams.

prepared by different quenching method are near the regression line of PLLA as well as in the graph of Young's modulus (Fig. 7). The relative elastic limit stress of PLLA foams mainly depends on the relative density and depends less on the cell size (Figs. 1 and 2) as well as Young's modulus. The values of σ_{el}/E_s of PLLA, PCL, and PHBV at a relative density of 1.0 were 0.067, 0.073, and 0.032, respectively.

Zhang et al. also showed that the elastic limit stress of the porous scaffolds with cubic and spherical macropores of PLGA were proportional to the power low. The exponents of the macroporous foams with spherical and cubic pores were 2.29 and 2.72, respectively [9].

Morgan and Keaveny measured that the yield stress of human trabecular bones from different anatomic site (vertebra, proximal tibia, greater trochanter, and femoral neck) [21]. The exponent of the relationship of yield stress on density was 1.48–2.26 in compression tests. They also showed that the Young's moduli are almost proportional to the yield stress, suggesting that the moduli also increase proportionally to the square of the density.

Gibson and Ashby [16] summarized the mechanical properties of open cell polyurethane foams and cancellous bones and showed the exponents of the dependence of elastic limit (collapse) stress on the densities are around 2.0. The theoretical exponents of elastic limit stress to density for the ideal open-cell foams in a simple model are 2.0 as well as that of Young's modulus [16]. The typical value of σ_{el}/E_s of open cell foams at a relative density of 1.0 is 0.05. The values for the foams of PLLA, PCL, and PHBV (0.032–0.073) are close to 0.05 suggesting that the elastic properties of those biodegradable foams prepared by thermally induced phase separation method can be roughly estimated from the Young's modulus of solid polymer and relative densities.

4. Conclusions

The compressive Young's modulus (E) of microporous foams of PLLA, PCL, and PHBV prepared by thermally induced phase separation method was proportional to the relative density (ρ/ρ_s) to the power of 2.0–2.7. The modulus was dependent on the Young's modulus (E_s) of the solid materials as well as the density but less dependent on the pore size. The ratio of the elastic limit stress (σ_{el}) to the Young's modulus of the solid materials (σ_{el}/E_s) was proportional to the relative density (ρ/ρ_s) to the power of 2.1–2.4. The mechanical properties of the microporous foams of the biodegradable polyesters were similar to those of open-cell polyurethane foams and cancellous bones. The mechanical properties of biodegradable foams are useful in the design of scaffold in tissue engineering and support of drug delivery systems to obtain mechanical biocompatibilities of the foam to the site of implantation.

Acknowledgement

We thank Toyota Motor Corp. for the kind gift of PLLA. We appreciate Ms. Satoko Eguchi for her technical assistance. This study was partially supported by Grant from Eno Science Foundation, Grants-in-Aid for Scientific Research from Japan Society for the Promotion of Science (21560807), and Grant for Promotion of Niigata University Research Projects.

References

[1] P.X. Ma, Adv. Drug Deliv., 60 (2008) 184–198.
[2] R. Langner and J.P. Vancanti, Science, 260 (1993) 920–926.
[3] S. Yang, K. Leong, Z. Du and C. Chua, Tissue Eng., 7 (2001) 679–689.
[4] H. Lo, M.S. Ponticiello and K.W. Leong, Tissue Eng., 1 (1995) 15–28.
[5] M. Biondi, F. Ungaro, F. Quaglia and P.A. Netti, Adv. Drug Deliv., 60 (2008) 229–242.
[6] X. Liu and P.X. Ma, Biomaterials, 30 (2009) 4094–4103.
[7] A.G. Mikos, A.J. Thorsen, L.A. Czenwonka, Y. Bao, R. Langer, D.N. Winslow and J.P. Vacanti, Polymer, 35 (1994) 1068–1077.
[8] Q. Hou, D.W. Grijpma and J. Feijen, Biomaterials, 24 (2003) 1937–1947.
[9] J. Zhang, L. Wu, D. Jing and J. Ding, Polymer, 46 (2005) 4979–4985.
[10] L. Wu, J. Zhang, D. Jing and J. Ding, J. Biomed. Mater. Res., 76A (2006) 264–271.
[11] Q. Hou, D.W. Grijpma and J. Feijen, J. Biomed. Mater. Res., 67B (2003) 732–740.
[12] S.C. Baker, G. Rohman, J. Southgate, N.R. Cameron, Biomaterials, 30 (2009) 1321–1328.

[13] I. Zein, D.W. Hutmacher, K.C. Tan and S.H. Teoh, Biomaterials, 23 (2002) 1169–1185.
[14] F.P.W. Melchels, J. Feijen and D.W. Grijpma, Biomaterials, 30 (2009) 3801–3809.
[15] D.E. Discher, D.J. Mooney and P.W. Zandstra, Science, 324 (2009) 1673–1677.
[16] L.J. Gibson and M.F. Ashby, Cellular Solids – Structure & Properties, 2nd ed., Cambridge University Press, Cambridge, UK, 1997.
[17] D.R. Lloyd, S.S. Kim, K.E. Kinzer, J. Membr. Sci., 64 (1991) 1–11.
[18] T. Tanaka and D.R. Lloyd, J. Membr. Sci., 238 (2004) 65–73.
[19] T. Tanaka, T. Tsuchiya, H. Takahashi, M. Taniguchi, H. Ohara and D.R. Lloyd, J. Chem. Eng. Jpn., 39 (2006) 144–153.
[20] C.C. Han, J. Ismail and H.-W. Kammer, Polym. Degrad. Stab., 85 (2004) 947–955.
[21] E.F. Morgan and T.M. Keaveny, J. Biomech., 34 (2001) 569–577.